# Effects of Structural Factors on the π-Dimerization and/or Disproportionation of the Cation Radical of Extended TTF Containing Thiophene-Based π-Conjugated Spacers

**Pierre Frère,*[a] Magali Allain,[a] El Hadj Elandaloussi,[a] Eric Levillain,[a] François-Xavier Sauvage,[b] Amédée Riou,[a] and Jean Roncali[a]**

**Abstract:** The electrochemical and chemical oxidation of extended TTF **4** and **5** are analysed by cyclic voltammetry, Visible/NIR and ESR spectroscopies, and the X-ray structures of the new salts **5**·$BF_4(CH_2Cl_2)$ and **4**·$ClO_4(THF)_{1/2}$ are presented. The effects of structural factors on the π-dimerization or the disproportionation reaction of the cation radical are shown. The oxidation of compound **4** presents the successive formation of stable cation radical and dication species both in dichloromethane (DCM) and in a $CH_3CN$/THF mixture. In contrast, for compound **5**, the stability of the oxidation states strongly depends on the nature of the solvent. In DCM, the oxidation of **5** proceeds by two close one-electron transfers while in $CH_3CN$/THF the dication is directly formed via a two-electron process. The X-ray structures of the two salts reveal the formation of π-dimers of cation radical. While the dimer $(\mathbf{5}_2)^{2+}$ is due mainly to π–π interactions between the conjugating spacer, the multiplication of the sulfur atoms in compound **4** contributes to stabilize the dimer by the combined effects of S–S and π–π interactions. Visible/NIR and ESR experiments confirm the higher tendency of $\mathbf{4}^{+\cdot}$ to dimerize with the occurrence of dimer and monomer in solution, while for $\mathbf{5}^{+\cdot}$ only the monomer is detected in DCM. On the other hand, by dissolution of **5**·$BF_4(CH_2Cl_2)$ in $CH_3CN$, only the neutral and the dicationic states of compounds **5** are observed owing to the disproportionation reaction.

**Keywords:** cyclic voltammetry · π interactions · radical ions · thiafulvalene

## Introduction

π-Conjugated polymers and oligomers and the tetrathiafulvalene derivatives (TTF) lead to two distinct classes of conductive materials which have been subject to independent and parallel investigations during the past decades.[1] TTF-based molecular materials are in general characterised by the formation of stacks of donors in a mixed-valence allowing a delocalisation of the electrons and a conductivity along the overlapping axis.[2] For doped polymer such as polythiophene or polypyrrole, the electrical conductivity involves both an intra- and interchain charge transport, respectively, by delocalization of the charge along the conjugated system and by hopping of the carriers between neighbouring chains.[3] The mechanism invoked to explain the interchain transport suggests the existence of π-stacks and constitutes an analogy to the conductivity mode in the cation radical salt of TTF derivatives.[4] This hypothesis is supported by the discovery of the formation of the π-dimer of cation radical in oligothiophene or oligopyrrole.[5] Recently, X-ray structures of oxidised diphenyl-terthiophene **1a**[6] and diphenyl-bipyrrole **1b**[7] proved the existence of the π-stacks and π-dimers in the solid state and confirmed the strong similarity of the structure of molecular materials derived from oxidised short-chains conjugated oligomers and TTF analogues. On the other hand, the consequences of the dimerization on the optical and electronic properties of the two classes of materials are subject to considerable interest.[8]

In order to combine the specific properties of oligomers and TTF, hybrid molecules built by insertion of a linear π-conjugated system between two 1,3-dithiole cycles have been developed.[9] In function of the length of the spacer, these compounds can be considered either as extended analogues of TTF or as oligomers end capped by dithiafulvene groups. In presence of a very long oligothienylenevinylene spacer, the electronic properties dictated by the conjugated system are

[a] Prof. P. Frère, M. Allain, Dr. El H. Elandaloussi, Dr. E. Levillain, Prof. A. Riou, Dr. J. Roncali
Ingénierie Moléculaire et Matériaux Organiques, CNRS
UMR 6501, Université d'Angers
2 Bd Lavoisier, 49045 Angers (France)
Fax: (+33) 241 73 54 05
E-mail: pierre.frere@univ-angers.fr

[b] Dr. F.-X. Sauvage,
Laboratoire de Chimie-Physique LASIR-HEI, CNRS UMR 8516
13, rue de Toul, 59046 Lille Cedex (France)

Supporting information for this article is available on the WWW under http://www.wiley-vch.de/home/chemistry/ or from the author.



0947-6539/02/0804-0784 $ 17.50+.50/0 *Chem. Eur. J.* **2002**, *8*, No. 4

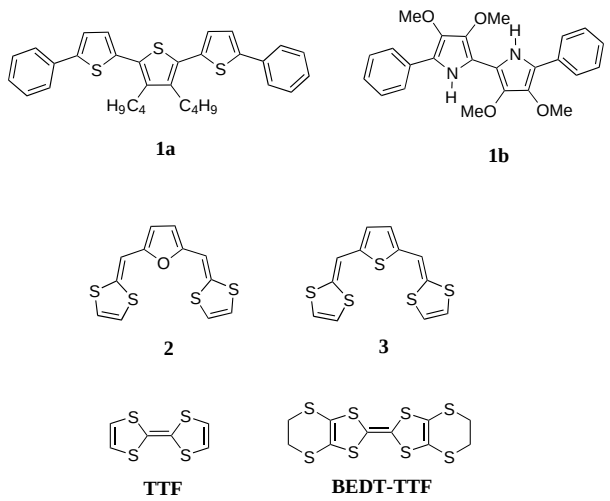


modulated by the dithiole cycles which increase the intermolecular interactions in the solid state.[10] While with a short spacer, the hybrid molecules lead to cation radical salts characterised by a π-stacking of the donors as currently observed for TTF derivatives.[11–12] We have recently shown that for compounds **2** and **3**, the overlapping strongly depended on the nature of the central heterocycle.[11] In particular, the thiophene cycle in **3** favours the formation of dimers owing to S···S intermolecular interactions between the sulfur atoms of the spacer while for **2** only weak S···O interactions between the heteroatoms of the spacer and the dithiafulvene cores were observed. In order to increase the intermolecular interactions in the materials, structural modifications of **3** have been designed. Two different approaches, according to that the substituents or the spacer are modified (Scheme 1), have been elaborated. In the former, the compound **4** has been built by addition of ethylenedithio groups to the dithiafulvene cycles by analogy with the well known bis-ethylenedithio-TTF (BEDT-TTF, see above). In fact, the prominent role of the peripheral sulfur atoms in the formation of bidimensionnal materials by the multiplication of the intermolecular S···S interactions has been evidenced.[13] In the second approach, the spacer has been lengthened in order to increase the π–π interactions as observed for conjugated oligomers. To avoid the torsion of the spacer associated with the presence of dithiafulvene groups grafted on a short oligothiophene,[14] the more rigid thienylenevinylene system[15] has been chosen in the design of hybrid-TTF **5**. The formation of the π-stacks and π-dimers in solution of oligothienylenevinylene has recently been described.[16]

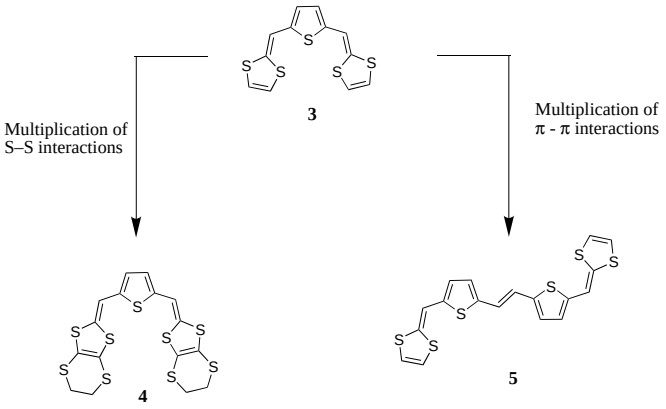


Scheme 1.

**Abstract in French:** *L'oxydation électrochimique ou chimique des analogues étendus du TTF **4** et **5** a été étudiée par voltamétrie cyclique et par spectroscopies Visible/proche-IR et RPE. La corrélation de la structure des radicaux cations et de leur aptitude à dimériser ou à se dismuter est discutée. En solution dans le dichlorométhane (DCM) ou dans un mélange acétonitrile/tétrahydrofuranne ($CH_3CN$/THF), le composé **4** s'oxyde réversiblement en cation radical puis en dication. La présence d'un système conjugué plus étendu pour le composé **5** facilite l'accès au dication. Ainsi l'oxydation de **5** s'effectue en deux étapes monoélectroniques très proches dans le DCM, tandis qu'une seule étape à deux électrons est observée dans le mélange $CH_3CN$/THF. Des monocristaux des sels **5**·$BF_4(CH_2Cl_2)$ et **4**·$ClO_4(THF)_{1/2}$ ont été analysés par diffraction des rayons X. La structure des sels révèle la formation de dimères de radicaux cations. Pour le composé **4**, enrichi en atome de soufre, les dimères $(\mathbf{4}_2)^{2+}$ sont stabilisés à la fois par des interactions π–π et des interactions soufre–soufre. En solution dans le dichlorométhane ou l'acétonitrile, la présence de dimère est observée. Pour le composé **5** le processus de dimérisation est principalement dû à des interactions π entre les systèmes conjugués. En solution dans le dichlorométhane, seule la présence de radicaux cations est détectée, tandis que dans l'acétonitrile, ces derniers se dismutent en dications et donneurs neutres.*

We report here on the preparation and the investigations on the molecular and crystal structures of the new salts namely **4**·$ClO_4(THF)_{1/2}$ and **5**·$BF_4(CH_2Cl_2)$ in which π-dimer of cation radical are observed. In particular, we show the influence of the conjugated linear system or the dithiafulvanyl groups on the formation of the dimers. In solution, we present a detailed investigation of the stability of the redox states of the extended TTF **4** and **5**. Both the structure of the donor and the nature of the solvent play an essential role in the tendency to form a dimer in solution or to favour the disproportionation reaction of the cation radical.

## Results and Discussion

**Electrochemistry of compounds 4 and 5**: Compound **4** has been synthesised as already described.[17] Compound **5** was obtained in 20% yield by a thermal demethoxycarbonylation of **6**[15] in HMPA in presence of LiBr, $H_2O$ (Scheme 2).

The cyclic voltammograms (CV) of **4** and **5** in dichloromethane (DCM) and THF/$CH_3CN$ (1:2) mixture (the solubility of **4** and **5** in $CH_3CN$ is too low) are shown Figure 1 and the data are listed in Table 1.

In DCM, the CV of **4** presents two reversible oxidation waves with peaks at $E_{pa1} = 0.41$ V and $E_{pa2} = 0.58$ V

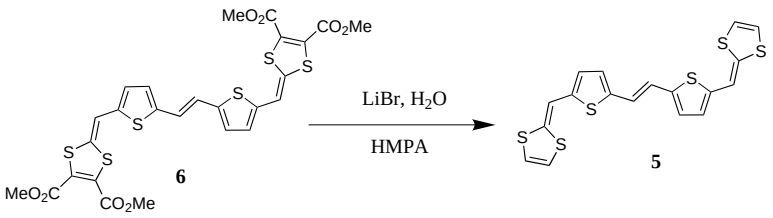


Scheme 2.

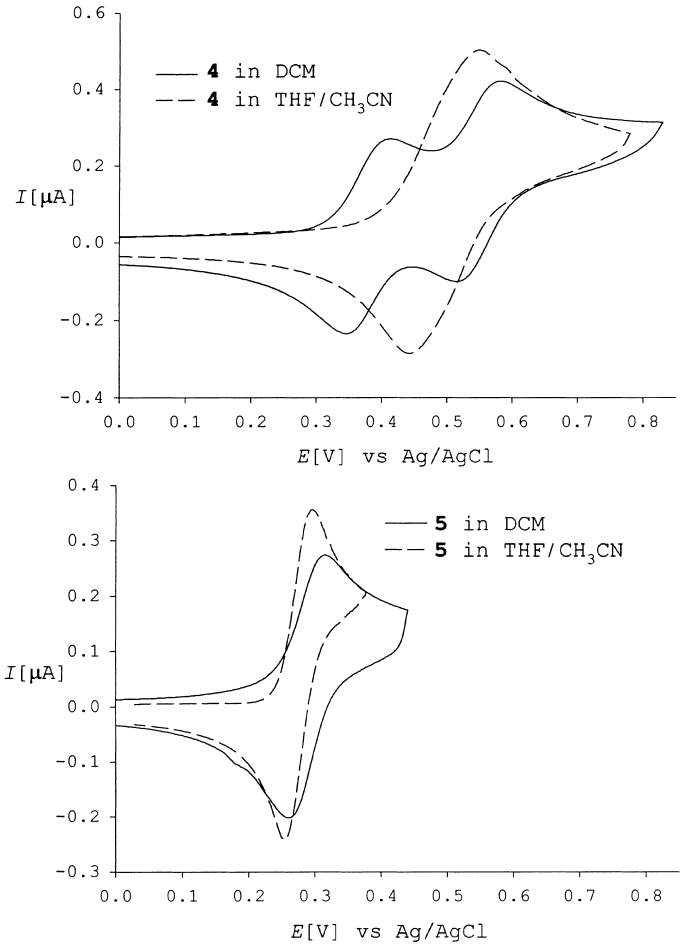


Figure 1. Cyclic voltammograms of compounds **4** (top) and **5** (bottom); $5\times10^{-4}$ mol L$^{-1}$ with $Bu_4NPF_6$ (0.1M) in DCM or THF/$CH_3CN$; scan rate 100 mV s$^{-1}$; reference Ag/AgCl.

Table 1. Electrochemical data of compounds **4** and **5**.

| **4** | $E_{ox1}$ [V] | $E_{ox2}$ [V] | $\Delta E$ [mV] | $K$ |
|---|---|---|---|---|
| DCM | 0.41 | 0.58 | 170 | $1.3\times10^{-3}$ |
| THF/$CH_3CN$ | 0.48 | 0.55 | 70 | $6.5\times10^{-2}$ |
| **5** | $E_{ox}$ [V] | Peak[a] | $\Delta E$ [mV] | $K$ |
| DCM | 0.32 | 50 mV | 15 | 0.55 |
| THF/$CH_3CN$ | 0.29 | 30 mV | 0 | |

[a] Peak width at half maximum.

corresponding to the successive generation of radical cation and dication. In THF/$CH_3CN$, the CV shows a strong decrease of the potential difference $\Delta E = E_{pa2} - E_{pa1}$ from 170 to 70 mV. Considering the disproportionation reaction of cation radical into neutral and dication shown below, the relative thermodynamic stability of the cation radical corresponding to a low value of the equilibrium constant $K$ [Eq. (1)], can be calculated from the potential difference with the Equation (2).[18]

The decrease of $\Delta E$, corresponds to a larger value of $K_{THF/CH_3CN} = 6.5\times10^{-2}$ ($K_{DCM} = 1.3\times10^{-3}$) indicating a lower

$$2\,\mathbf{D}^{+\cdot} \rightleftarrows \mathbf{D} + \mathbf{D}^{2+}$$

with

$$K = \frac{[\mathbf{D}]\,[\mathbf{D}^{2+}]}{[\mathbf{D}^{+\cdot}]^2} \quad (1)$$

and

$$K = \exp\left[\frac{F}{RT}(-\Delta E)\right] \quad (2)$$

thermodynamic stability of the radical cation in this solvent. As already described for BEDT-TTF[19] and TTF vinylogues,[20] polar solvent such as $CH_3CN$ stabilize the dication to the detriment of the cation radical by solvation effects. In other words, these solvents favour the disproportionation reaction. Electrocrystallization of **4** under galvanostatic conditions performed in DCM only led to a green solution while in presence of THF (10% volume) single crystals with the stoechiometry **4 · ClO$_4$(THF)$_{1/2}$** was obtained.

For **5**, the choice of the solvent plays a major role on the oxidation state reached during the electrocrystallizations. The CV of **5** in DCM shows a reversible oxidation wave at 0.33 V corresponding to the formation of the dication. The peak width at half maximum (PWHM) of 50 mV is larger than the 28.5 mV expected for an ideal two-electron transfer;[21] this suggests that the oxidation process involves two very close one-electron steps ($\Delta E = 15$ mV). As expected, the lengthening of the spacer allows a stabilization of the dicationic state by decreasing the intramolecular coulombic repulsion and favours the disproportionation reaction as indicated by the value of $K_{DCM} = 0.55$. However, some electrocrystallizations performed in DCM under galvanostatic condition led to salts of stoichiometry **5 · BF$_4$(CH$_2$Cl$_2$)** or **5 · ClO$_4$(CH$_2$Cl$_2$)** in which cation radicals are associated in dimers (see below). Thus, the further stabilization of the cation radical by dimerization in the solid, allows to isolate the little stable +1 oxidation state of **5**.

In THF/$CH_3CN$, the PWHM reaches 30 mV indicating a direct oxidation to the dication. The combination of the long spacer with the strong solvation effect of $CH_3CN$ allows an easy access to the more stable dicationic state and inhibits the formation of the radical cation. The localization of the positive charges of the dication at the ends of the molecule minimizes the coulombic repulsion and enhances the interactions with the solvent thus allowing the potential inversion.[22] Some electrocrystallizations of **5** performed in this solvent either under galvanostatic conditions at low current or



0947-6539/02/0804-0786 $ 17.50+.50/0 *Chem. Eur. J.* **2002**, *8*, No. 4

at constant potential (0.35 V) led to powders corresponding to the dication salts.

**Structures of the +1 oxidation state of compounds 4 and 5 in the solid phase**: The stoichiometry and structure of the salts have been determined by single-crystal X-ray analysis. **4·ClO$_4$(THF)$_{1/2}$** crystallizes in the *P*bca space group. The structure consists of two independent molecules namely **4a** and **4b**, two $ClO_4^-$ anions and a molecule of solvent.

As shown in Figure 2, both **4a** and **4b** adopt a *syn* conformation stabilised by two strong S···S intramolecular interactions. The non-bonded length with a distance about 3.05 Å are much shorter than the sum of the van der Waals radii ($r_S = 1.85$ Å) but larger than a covalent S–S single bond (2.04 Å). Such 1,5-intramolecular interactions, already observed for **3** in both the radical cation and the neutral molecule, contribute to the planar conformation of the donors in these various oxidation states.[11] For **4a** and **4b**, the molecules are quite planar except for the carbon atoms of the ethylenedithio groups. The torsion angle between the dithiafulvenyl arms and the central thiophene cycle is smaller than 5°. The THF molecule, located in the interstice of **4a**, is stabilised by two S···O contacts with distances 3.43 and 3.47 Å between the sulfur atoms of the 1,3-dithiole rings and the oxygen atom of the solvent.

The structure of **4·ClO$_4$(THF)$_{1/2}$** is characterised by the formation of dimers **(4$_2$)$^{2+}$** with a face-to-face stacking of monomers. The intermolecular distances between the sulfur and the carbon atoms of the monomers are reported in Table 2. The numerous S···S intermolecular contacts close to the van der Waals distance (3.7 Å) shows that, as for dimers of BEDT-TTF,[23] the sulfur atoms of the dithiafulvalenyl groups contribute to the formation of the dimer. On the other hand, short intermolecular contacts are observed for the carbon atoms of the spacer (less than 3.5 Å) in particular those for thiophene carbons, the shortest distances are close to 3.14 Å and 3.23 Å. Such distances which are characteristic for a π-dimer are smaller than those observed in the recently described **(1b$_2$)$^{2+}$**dimer.[7]

Table 2. Interatomic distances in the dimer **(4$_2$)$^{2+}$**.

| S–S [Å] | | C–C [Å] | | Lateral C–C [Å] | |
|---|---|---|---|---|---|
| S1A – S1B | 3.644(8) | C1A – C1B | 3.60(3) | C2A – C1B | 3.28(3) |
| S2A – S2B | 3.869(9) | C2A – C2B | 3.41(3) | C4A – C3B | 3.14(3) |
| S3A – S3B | 3.575(9) | C3A – C3B | 3.42(3) | C5A – C6B | 3.23(3) |
| S4A – S4B | 4.11(1) | C4A – C4B | 3.23(3) | C7A – C8B | 3.41(3) |
| S5A – S5B | 3.80(1) | C5A – C5B | 3.31(3) | | |
| S6A – S6B | 3.598(8) | C6A – C6B | 3.47(3) | | |
| S7A – S7B | 3.638(9) | C7A – C7B | 3.50(3) | | |
| S8A – S8B | 3.63(1) | C8A – C8B | 3.54(3) | | |
| S9A – S9B | 3.71(1) | | | | |

These results suggest that the formation of the **(4$_2$)$^{2+}$** dimer results from the combination of two types of factors namely the strong S···S interactions associated with the dithiafulvenyl groups as for TTF derivatives and the overlap of the π-orbitals of the carbon atoms of the conjugated spacer as described for π-dimers of short-chain oligothiophenes or oligopyrroles. The strong dimerization of the radical cation in the solid state is confirmed by the absence of ESR signal of **4·ClO$_4$(THF)$_{1/2}$** due to the spin pairing in the dimer.

The association of the dimers are presented in Figure 3. Along the [1,0,0] axis, the dimers stack with a shift of molecules presenting weak interactions with a interplanar contact distances about 3.7 Å. On the other hand, as shown in Figure 3 (bottom) the dimers are connected in the [0,0,1] direction by short S···S contacts of 3.50(1) and 3.52(2) Å between the ethylenedithio groups and the dithiole cycles forming sheets of dimers. The anions and the molecules of THF are inserted between the cation in the direction [0,1,0] separating the sheets of dimers.

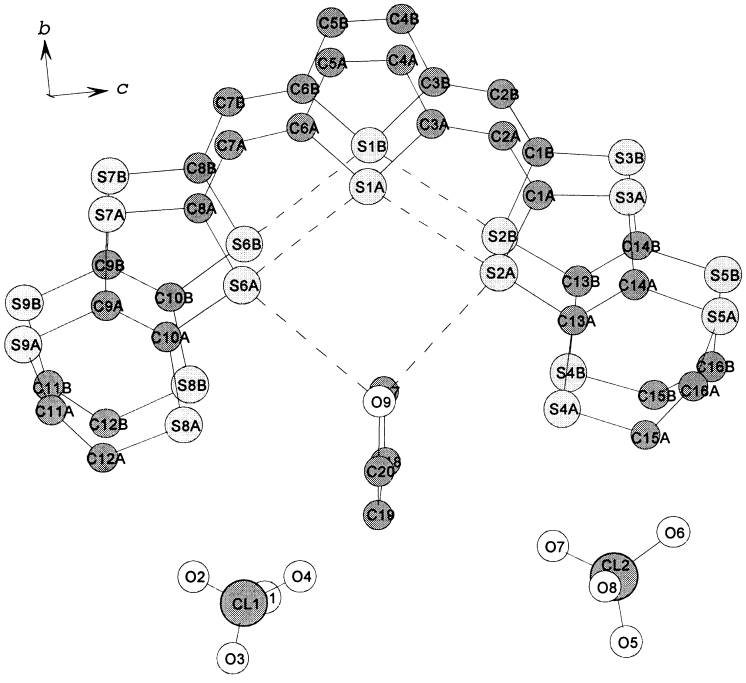


Figure 2. Molecular structure of dimer **(4$_2$)$^{2+}$** showing the S···S intramolecular interactions and S···O contacts with the solvent.

The visible/NIR spectrum of **4·ClO$_4$(THF)$_{1/2}$** at room temperature (Figure 4, top) shows two main bands at 690 and 1110 nm assigned to the absorption band D1 and D2 of the dimeric cation radical **(4$_2$)$^{2+}$**. In addition, the optical conductivity band due to the charge-transfer between the dimers is observed in the NIR range. Two-probe conductivity measurements performed on a single crystal gave a value of $10^{-3}$ S cm$^{-1}$, a value two orders of magnitude larger than that of cation radical salt for compound **3**.[10] The presence of the peripheral sulfur atoms in **4** contributes to the multiplication of the intermolecular contacts increasing the dimension-

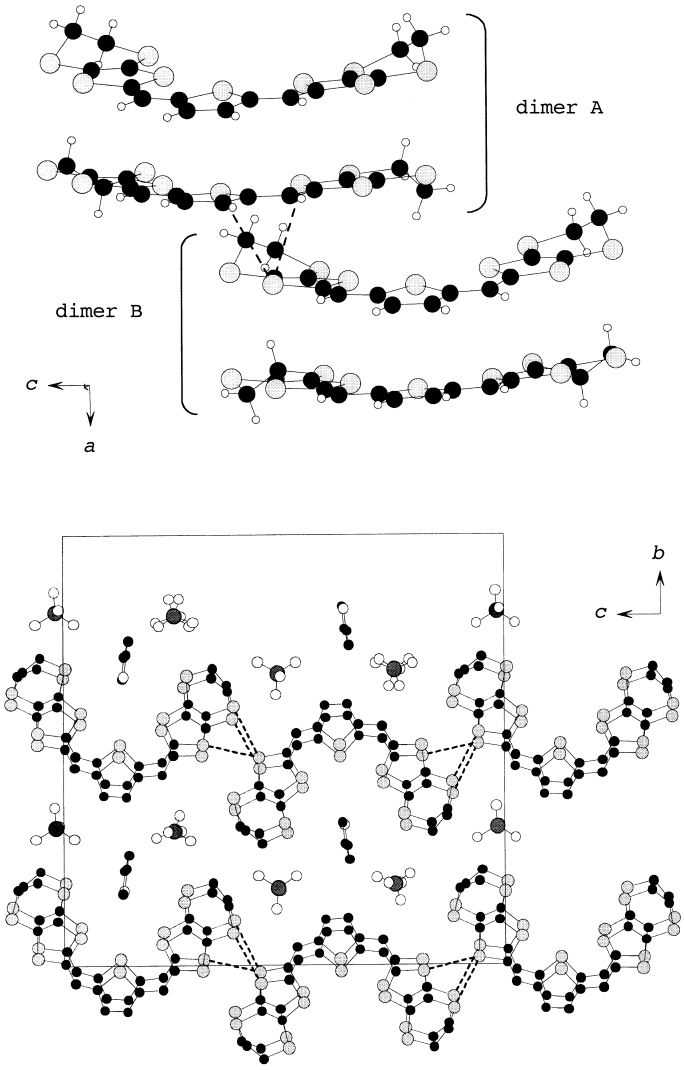


Figure 3. Sulfur–Sulfur interactions between the dimers in the salt **4·ClO$_4$(THF)$_{1/2}$**.

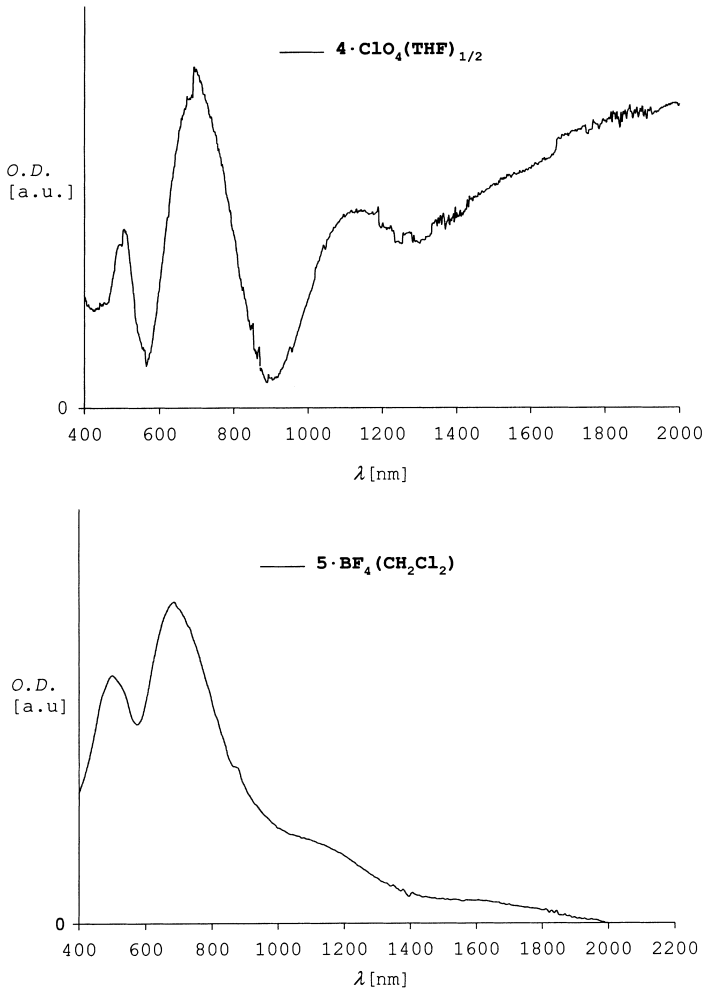


Figure 4. Visible/NIR spectra of the salts **4·ClO$_4$(THF)$_{1/2}$** (top) and **5·BF$_4$(CH$_2$Cl$_2$)** (bottom) in the solid state.

ality of the materials and thus its conductivity as proven by extended and sulfur-rich analogues of TTF.[24]

Compounds **5·BF$_4$(CH$_2$Cl$_2$)** and **5·ClO$_4$(CH$_2$Cl$_2$)** are isostructural and crystallize in the *P*bca group. The structures consist of a donor, an anion and a molecule of $CH_2Cl_2$. At 293 K, while the position of the donor is well defined, the solvent and the anions present a strong thermal disorder especially for $BF_4^-$. Consequently, for **5·BF$_4$(CH$_2$Cl$_2$)**, the refinement did not allow to reach a low value for *R* owing to the position of the anion which could not be determined without fixing the thermal parameters for the fluorine and boron atoms. In addition, the chlorine atoms of the solvent oscillate between two positions. The X-ray structure of **5·BF$_4$(CH$_2$Cl$_2$)** determined at 125 K has allowed to fix the position of the chlorine and boron atoms improving the resolution of the structure. Nevertheless, the motion of the anion corresponding to a rotation around the B–F1 axis was always observed.

The crystal structure reveals that the donors present the *syn* conformation of the dithiafulvalenyl groups stabilised by two strong S···S intramolecular interactions as indicated in Figure 5 by the short non-bonded contact with distances 3.039(3) and 3.092(3) Å. These interactions contribute to the planarity of the molecule for which the torsion angle between the dithiafulvalenyl arms and the plane of the central thienylenevinylene system is close to 2°. The structure is characterised by the formation of dimers $(\mathbf{5_2})^{2+}$ separated in the [1,0,0] direction by the anions and the solvent. A similar structure, where no stacking of the dimer is possible due to the intercalation of the anions, has recently been described for oligomer **1b** and explains no ESR activity.[7] The various intermolecular distances observed for the superposition of cations at $T = 125$ K are reported in Table 3. The strongest S···S interaction $d = 3.400(4)$ Å involves the sulfur atom of the 1,3-dithiole cycles while the distance between the sulfur atoms of the thiophene cycles is only of 3.676(4) Å. Concerning the C···C intermolecular contacts, the shorter bond lengths C3–C11, C6–C10 and C7–C8, close to 3.35 Å, involve the carbons of the thienylenevinylene spacer and correspond to the overlaps of the π-orbitals. The contribution of the sulfur–sulfur interactions of $(\mathbf{5_2})^{2+}$ to stabilize the dimers is less important than in $(\mathbf{4_2})^{2+}$ showing that the dimerization of TTF analogues with long conjugated spacer is closer to that of conjugated oligomers than that of TTF derivatives.



0947-6539/02/0804-0788 $ 17.50+.50/0 *Chem. Eur. J.* **2002**, *8*, No. 4

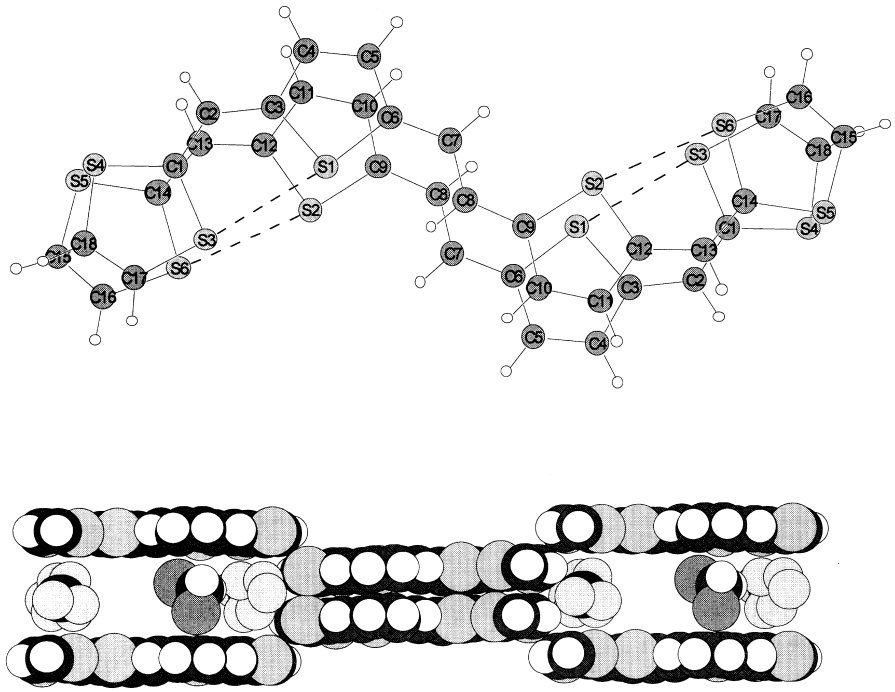


Figure 5. Molecular structure of $(\mathbf{5}_2)^{2+}$ and packing of the dimers.

Table 3. Interatomic distances in the dimer $(\mathbf{5}_2)^{2+}$.

| S–S [Å] | | C–C [Å] | | Lateral C–C [Å] | |
|---|---|---|---|---|---|
| S1–S2 | 3.676(4) | C1–C14 | 3.53(1) | C1–C13 | 3.48(1) |
| S6–S3 | 3.662(4) | C2–C13 | 3.45(1) | C3–C11 | 3.35(1) |
| S4–S5 | 3.400(4) | C3–C12 | 3.50(1) | C6–C10 | 3.32(1) |
| | | C4–C11 | 3.41(1) | C8–C8 | 3.35(1) |
| | | C5–C10 | 3.48(1) | | |
| | | C6–C9 | 3.57(1) | | |
| | | C7–C8 | 3.60(1) | | |

Comparison with the structures determined at 293 K both in the presence of $BF_4^-$ or $ClO_4^-$ anions shows that the interactions in the dimers weakly depend on the temperature. Thus, the interplanar distance between the planes formed by the thiophene cycles in the spacer only decreases from 3.45(5) Å at 293 K to 3.35(1) Å at 125 K.

The visible/NIR spectrum of $\mathbf{5 \cdot BF_4(CH_2Cl_2)}$ (Figure 4 bottom) exhibits an intense and broad band at 730 nm with a shoulder around 1200 nm assigned to the D1 and D2 absorption of the dimer $(\mathbf{5}_2)^{2+}$. Contrary to the previous salt, the optical conduction band is very weak indicating a poor charge-transfer between the dimers. This behaviour is consistent with the insulating character of the salt and with the weak contacts among the dimers indicated by the X-ray structure.

**Stability of the oxidation states of compounds 4 and 5 in solution**: The stability of the different species (monomer or dimer of cation radical and dication) resulting from the oxidation of compounds **4** and **5** in DCM or $CH_3CN$ solutions were examined by visible/NIR and ESR spectroscopies.

The visible/NIR spectra of a solution of **4** ($5 \times 10^{-4}$ M) in DCM at room temperature recorded during the stepwise addition of a $NOBF_4$ solution are shown in Figure 6. The oxidation of **4** into cation radical is marked by a decreasing of the the neutral state band at 465 nm and by two new main bands at 743 and 1310 nm (M1 and M2) with shoulders at 670 and 1120 nm, respectively. By addition of an excess of oxidant, the bands of the cation radical are replaced by a band at 480 nm and a weak broad band at 750 nm assigned to the dication.

The $\mathbf{4 \cdot ClO_4(THF)_{1/2}}$ salt is weakly soluble in DCM leading to a green solution which gives the same spectrum obtained by addition of one equivalent oxidant to a solution of **4**. In $CH_3CN$, the spectrum is very similar with a blue shift of the bands but the resulting solution

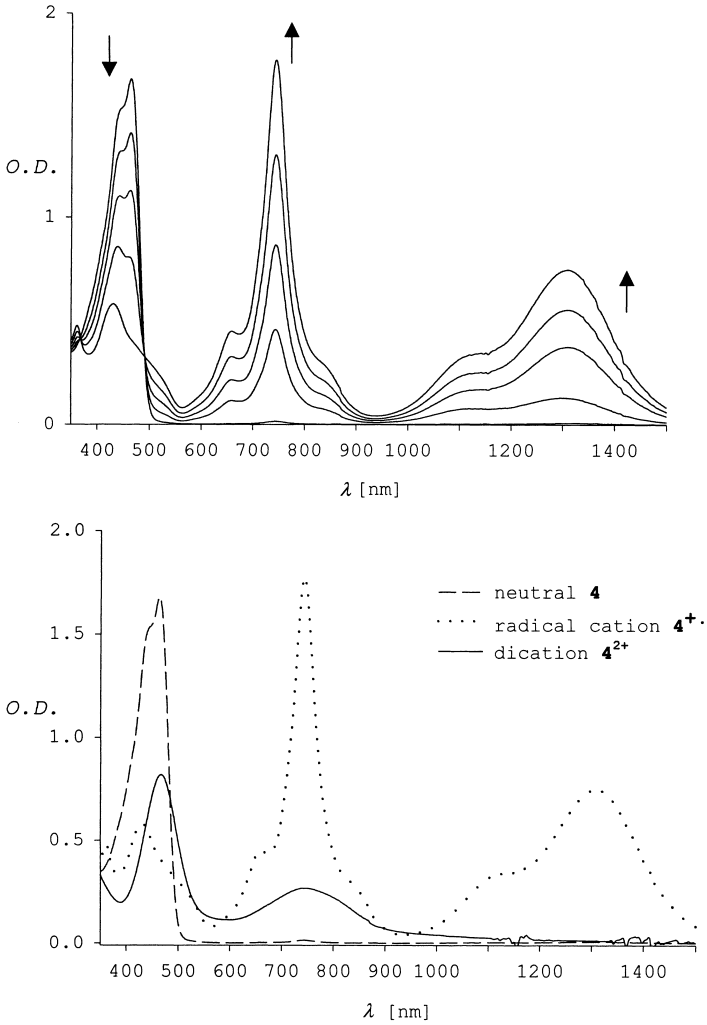


Figure 6. Chemical oxidation of compound **4** in DCM.

is less stable and the green colour vanishes after a few time (about 30 min). The use of a saturated solution of **4** (about $10^{-3}$ M) results in a relative intensification of the bands at 670 nm (D1) and 1120 nm (D2) (Figure 7). This concentration effect and the comparison with the absorption in the solid state indicates that D1 and D2 correspond to the dimers of the cation radical $(\mathbf{4}_2)^{2+}$ in solution while M1 and M2 are due to the monomeric species $\mathbf{4}^{+\bullet}$. The relative concentration of the dimer increases at higher substrate concentration but remains the minor species in solution. Addition of small amounts of THF to the solution lead to the precipitation of a salt giving the same spectrum as **4·ClO$_4$(THF)$_{1/2}$** in which only the dimer is present.

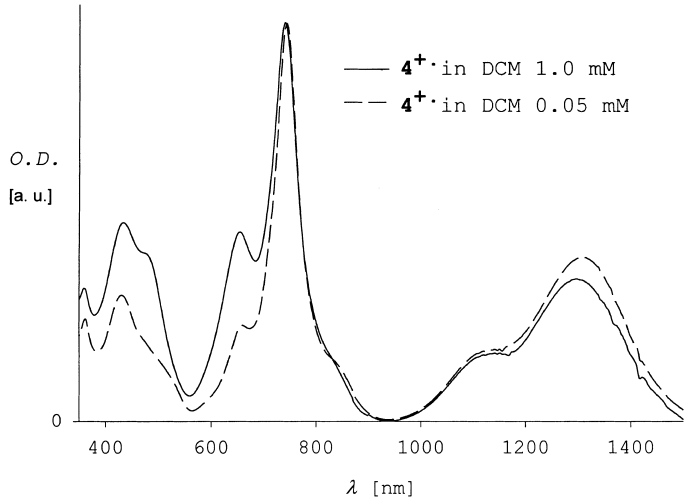


Figure 7. Visible/NIR spectra of cation radical $\mathbf{4}^{+\bullet}$ at 0.05 mM and 1 mM in DCM.

The dimerization equilibrium in the +1 oxidation state of compound **4** has been also confirmed by ESR spectroscopy. The ESR spectra of the **4·ClO$_4$(THF)$_{1/2}$** solution in DCM or $CH_3CN$ give a signal characteristic of the radical cation $\mathbf{4}^{+\bullet}$ in the solution. By cooling the sample from 298 to 263 K, the ESR signal intensity decreases; the change with the temperature is partially reversible after a fast warming of the solution. These results are consistent with a decrease of the spin population at low temperature due to a π-dimerization of cation radical rather than a precipitation of the salt because the monomer–dimer equilibrium is faster than the solid–solute equilibrium and is a reversible process. As expected for the exothermic equilibrium of dimerization, the formation of the spinless dimer is favoured at low temperature.

Compared with compound **4**, solutions of the +1 oxidation state of **5** presents a dramatically different behaviour of the ESR and visible/NIR spectra. The ESR spectrum of a DCM solution of **5·BF$_4$(CH$_2$Cl$_2$)** shows a signal with the intensity which increases upon cooling. This classic variation of the signal intensity by a Curie's law shows that the radical cation $\mathbf{5}^{+\bullet}$ does not dimerize at lower temperatures. In addition, the electronic spectrum of this solution shows only two bands at 890 and 1560 nm assigned to the monomeric cation radical $\mathbf{5}^{+\bullet}$, while the presence of the dimeric species for **5** is not detectable in the solution. By comparison with compound **4**, the strong stabilization of the dimer $(\mathbf{4}_2)^{2+}$ due to both S···S and π–π interactions allows for the dimers in solution while the weak interactions observed in $(\mathbf{5}_2)^{2+}$ leads to a less stable dimer which dissociates into two cation radicals in solution.

Contrary to the previous results, the ESR spectrum of **5·BF$_4$(CH$_2$Cl$_2$)** in $CH_3CN$ presents a very weak signal. If this effect can be interpreted by a dimerization of the cation radical, it is also possible to consider the disproportionation reaction of the radical cation which leads to spinless neutral and dication species of **5**. In addition this last hypothesis is supported by the UV/Vis spectrum of the $CH_3CN$ solution of **5·BF$_4$(CH$_2$Cl$_2$)** which has two main absorption bands at 480 and 745 nm corresponding to the superposition of the spectra of the neutral compound **5** and the dication $\mathbf{5}^{2+}$. In order to know the relative stability of the cation radical $\mathbf{5}^{+\bullet}$ in DCM or $CH_3CN$ the evolution of the electronic spectra recorded during the stepwise chemical oxidation of **5** have been examined and are presented in Figure 8. Addition of up to one equivalent $NOBF_4$ in a DCM solution of **5** leads to the formation of the M1 and M2 bands at 890 and 1580 nm related to the radical cation but also to a strong band at 745 nm. The latter band increasing to the detriment of M1 and M2 by further addition of the oxidant can be attributed to the dication $\mathbf{5}^{2+}$. Hence before the addition of one equivalent of oxidant, the neutral compound **5** and the two oxidation states $\mathbf{5}^{+\bullet}$ and $\mathbf{5}^{2+}$ are simultaneously present which is a clear indication of the disproportionation equilibrium of $\mathbf{5}^{+\bullet}$ in DCM.

In $CH_3CN$, the addition of a small amount of oxidant gives the band of the dication indicating that the oxidation proceeds by a two-electron transfer. The weak absorption at 880 nm which disappears after addition of two equivalents of oxidant can be assigned to a trace of radical cation in the $CH_3CN$ solution. Consistent with the electrochemical results, the +1 oxidation state of **5** is unstable in $CH_3CN$ and undergoes the disproportionation reaction.

## Conclusion

The electrochemical and chemical oxidation of extended TTF **4** and **5** and the X-ray structures of salts **5·BF$_4$(CH$_2$Cl$_2$)** and **4·ClO$_4$(THF)$_{1/2}$** have been described. The effects of the structure to orient the cation radical towards a π-dimerization or a disproportionation reaction have been shown.

The sulfur-rich compound **4** presents numerous S···S interactions in addition of the π–π interactions developed by the thiophene cycle strongly stabilizing the dimers in the solid state but also in solution. Moreover, the peripheral sulfur atoms increase the dimensionality of the materials.

For compounds **5**, the dithiafulvenyl groups end-capped to a longer conjugated spacer allow for an easier access to a dication state. In DCM the cation radical is trapped by precipitation and stabilised by the formation of dimers. The dimerization process is mainly driven by the conjugated system and only a weak participation of the sulfur atoms is observed. In $CH_3CN$, a further stabilization of the dication by



0947-6539/02/0804-0790 $ 17.50+.50/0 *Chem. Eur. J.* **2002**, *8*, No. 4

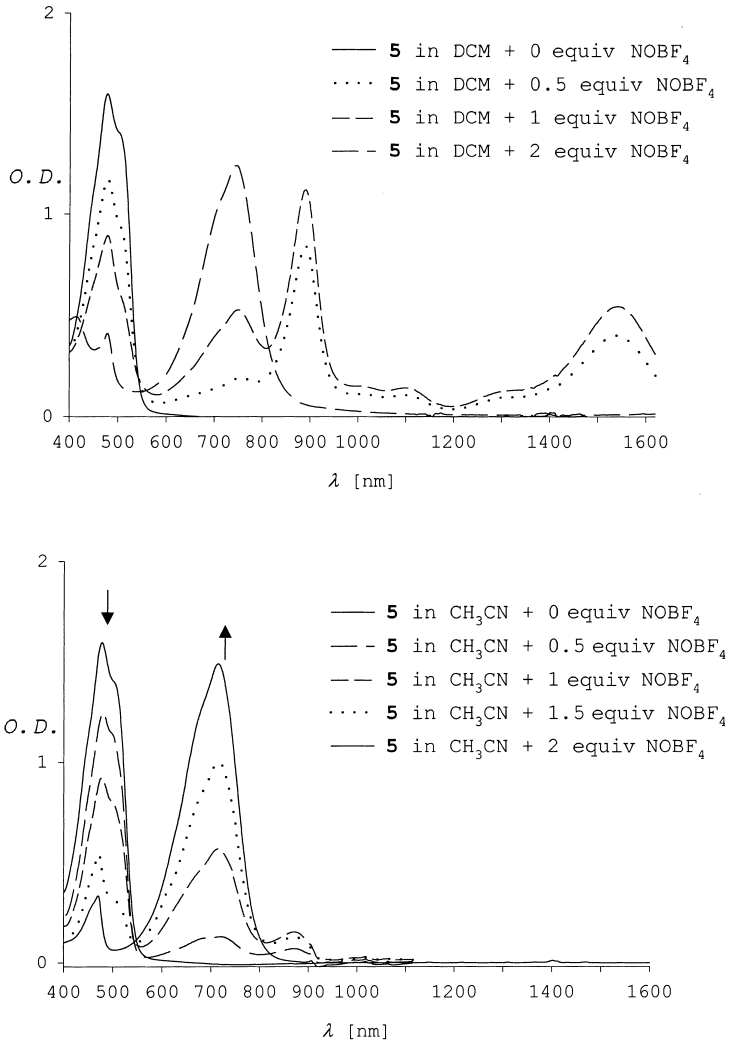


Figure 8. Chemical oxidation of compounds **5** in DCM (top) and $CH_3CN$ (bottom).

solvation leads to an inversion of the potential inhibiting the formation of the cation racical.

This work confirms the strong similarity between the structure of the molecular materials of oligomers and extended TTFs and reveals the major role of the heteroatoms as a control the intermolecular contacts propitious to a better mobility of the charge carriers.

## Experimental Section

**Synthesis of compound 5**: A solution of **6** (0.310 g, 0.5 mmol) and LiBr (1.12 g, 13 mmol) in HMPA (15 mL) was heated at 90 °C for 1 h, then 20 min at 120 °C. The reaction mixture was poured into water (60 mL) and extracted with $CH_2Cl_2$ ($2 \times 100$ mL). After drying over $MgSO_4$, the solvent was evaporated under reduce pressure and the residual oil was purified by column chromatography on silica gel ($CH_2Cl_2$ as eluent) to provide a red solid which was recrystallised from $CHCl_3$ (0.045 g, 20%). M.p. 258 °C (decomp); MS (EI): *m/z*: calcd for $C_{18}H_{12}S_6$: 419.92632; found: 419.9279; $^1$H NMR ($CDCl_3$, TMS): $\delta = 7.19$ (d, $^3J = 3.5$ Hz, 2H), 7.05 (d, $^3J = 3.5$ Hz, 2H), 7.01–6.98 (m, 4H), 6.95 (s, 2H), 6.91 (s, 2H).

**Electrochemical measurements**: Cyclic voltammetry was performed in a three-electrode cell (5 mL) equipped with a platinium millielectrode of $7.85 \times 10^{-3}$ cm$^2$ area and a platinium wire counter electrode. An Ag/AgCl electrode checked against the ferrocene/ferricinium couple before and after each experiment was used as reference. The electrolytic media involved $CH_2Cl_2$ (HPLC grade) or a mixture of tetrahydrofurane/acetonitrile (HPLC grade) and $5 \times 10^{-1}$ mol L$^{-1}$ of tetrabutylamonium-hexafluorophosphate (TBAHP, Fluka puriss). All experiments were carried out in solutions which were deaerated by argon bubbling at 298 K. Electrochemical experiments were carried out with an EGG PAR 273 A potentiostat with positive feedback compensation. Based on repetitive measurements, absolute errors on potentials were found to be around ±5 mV.

**Electrocrystallization**: Donors (about 5 mg) were dissolved in degassed solvent (40 mL) containing the electrolyte support ($10^{-1}$ mol L$^{-1}$) and placed in the anode compartment of H-shaped electrocrystallization cell, separated from the cathode compartment by a porous glass frit. A constant current of 1 $\mu$A was applied for 10 days at room temperature between the two platinum electrodes (wire: 0.5 mm diameter and 1.5 cm length). Crystals of cation radical salt grew on the anode were collected and washed with the solvent.

**Electronic absorption measurements**: UV/Vis/near-IR experiments have been performed with Perkin–Elmer Lambda 19 NIR spectrometer. Solvents (HPLC grade) were dried and deoxygenated before use. Quartz cells of 10 mm or 1 mm were used in function of the concentration of the donors ($5 \times 10^{-5}$ or $10^{-3}$ M). The oxidation of the neutral donors in solution was accomplished by adding solutions of nitrosonium tetrafluroborate ($NOBF_4$) from a micro-syringe.

**ESR studies**: ESR experiments were carried out on a Bruker ESP 300 spectrometer driven by Bruker ESP 1600 software. Experiments were performed in the X-band frequency range (≈9.4 GHz) in a TE102 cavity. The cells were made of silica (O.D. 3 mm). Low temperature measurements involved a standard variable-temperature cryostat using liquid nitrogen evaporation. The samples were prepared in a glove box containing dry, oxygen-free (< 1 vpm) argon. The experiments were done in the following way: First a spectrum was recorded at room temperature (298 K). The temperature was then lowered and subsequently the spectra were recorded. In order to make sure that the changes observed were not due to a precipitation of the solute, the temperature was then increased and new spectra recorded.

**X-ray crystallography**: Single crystals were mounted on an Enraf-Nonius MACH3 four circles diffractometer equipped with graphite monochromator and $Mo_{K\alpha}$ radiation ($\lambda = 0.71073$ Å).

The crystal structures were solved by direct methods (SIR) and refined on *F* by full matrix least squares techniques using MolEN package programs. The positions of hydrogen atoms were calculated from Hydro program. Crystal data and experimental details are listed in Table 4.

Crystallographic data (excluding structure factors) for the structure reported in this paper have been deposited with the Cambridge Crystallographic Data Centre as supplementary publication nos CCDC-167489 (**4·ClO$_4$(THF)$_{1/2}$**), -167490 (**5·BF$_4$(CH$_2$Cl$_2$)**) and -167491 (**5·ClO$_4$-(CH$_2$Cl$_2$)**). Copies of the data can be obtained free of charge on application to CCDC, 12 Union Road, Cambridge CB2 1EZ, UK (Fax: (+44) 1223-336-033; e-mail deposit@ccdc.cam.ac.uk).

Table 4. Crystallographic data.

| Compound | $4 \cdot ClO_4(THF)_{1/2}$ | $5 \cdot BF_4(CH_2Cl_2)$ | $5 \cdot ClO_4(CH_2Cl_2)$ |
|---|---|---|---|
| formula | $C_{36}H_{32}Cl_2O_9S1_8$ | $C_{19}H_{14}B_1Cl_2F_4S_6$ | $C_{19}H_{14}Cl_3O_4S_6$ |
| $F_w$ | 1256.71 | 592.42 | 605.05 |
| $T$ [K] | 294 | 125 | 294 |
| color | black | black | black |
| crystal system | orthorhombic | orthorhombic | orthorhombic |
| space group | *P*bca | *P*bca | *P*bca |
| $a$ [Å] | 13.971(4) | 36.44(1) | 36.83(1) |
| $b$ [Å] | 26.23(1) | 12.41(1) | 12.613(8) |
| $c$ [Å] | 26.75(1) | 10.289(3) | 10.493(3) |
| $V$ [Å$^3$] | 9803(1) | 4652(6) | 4874(5) |
| $Z$ | 8 | 8 | 8 |
| crystal size [mm$^3$] | $0.61 \times 0.42 \times 0.03$ | $0.31 \times 0.28 \times 0.14$ | $0.25 \times 0.19 \times 0.14$ |
| $\rho$ [g cm$^{-3}$] | 1.70 | 1.69 | 1.65 |
| $F(000)$ | 5136 | 2392 | 2456 |
| $\mu$ [mm$^{-1}$] | 0.951 | 0.855 | 0.915 |
| transmission min/max | 0.58/1.00 | 0.54/1.00 | 0.15/1.00 |
| $\theta$ range [°] | 2.5 to 24.97 | 2.5 to 20.93 | 2.5 to 21.10 |
| scan mode | $\omega/2\theta$ | $\omega$ | $\omega$ |
| index ranges | $0 < h < 16$ | $0 < h < 10$ | $0 < h < 10$ |
| | $0 < k < 31$ | $0 < k < 12$ | $0 < k < 12$ |
| | $0 < l < 31$ | $-36 < l < 0$ | $-37 < l < 0$ |
| data measured | 9061 | 2900 | 3062 |
| data independent | 9061 | 2872 | 3062 |
| data observed $I > 3\sigma(I)$ | 1989 | 1542 | 514 |
| variables | 361 | 216 | 129 |
| $R$ | 0.073 | 0.060 | 0.092 |
| $Rw$ [a] | 0.091 | 0.080 | 0.112 |
| largest peak in final difference [e Å$^{-3}$] | 0.961 | 1.425 | 0.553 |

[a] Weighting scheme: $w = 4F_o^2/[(\sigma(F_o^2))^2 + (0.08F_o^2)^2]$.


[1] a) *Handbook of Organic Conductive Molecules and Polymers*, *Vol. 1–4* (Ed.: H. S. Nalwa), Wiley, Chichester, **1997**; b) *Organic Conductors* (Ed.: J. P. Farges), Marcel Dekker, New York, **1994**; c) *Introduction to Synthetic Electrical Conductors* (Eds.: J. R. Ferraro, J. M. Williams), Academic, New York, **1987**.

[2] *Lower Dimensional System and Molecular Electronic*, *Vol. 1–3* (Eds.: R. M. Metzger, P. Day, G. C. Papavassiliou), Plenum, New York, **1990**.

[3] *Handbook of Conducting Polymers* (Eds.: T. A. Skotheim, R. L. Elsenbaumer, J. R. Reynolds), 2nd ed., Marcel Dekker, New York, **1998**.

[4] L. Miller, K. R. Mann, *Acc. Chem. Res.* **1996**, *29*, 417–423.

[5] a) Y. Yu, E. Gunic, B. Zinger, L. Miller, *J. Am. Chem. Soc.* **1996**, *118*, 1013–1018; b) J. A. E. H. van Haare, M. van Boxtel, R. A. J. Janssen, *Chem. Mater.* **1998**, *10*, 1166–1175.

[6] a) D. D. Graf, J. P. Campbell, L. Miller, K. R. Mann, *J. Am. Chem. Soc.* **1996**, *118*, 5480–5481; b) D. D. Graf, R. G. Duan, J. P. Campbell, L. Miller, K. R. Mann, *J. Am. Chem. Soc.* **1997**, *119*, 5888–5899.

[7] A. Merz, J. Kronberger, L. Dunsh, A. Neudeck, A. Petr, L. Parkanyi, *Angew. Chem.* **1999**, *111*, 1533–1538; *Angew. Chem. Int. Ed.* **1999**, *38*, 1442–1446.

[8] a) J. Cornil, D. Beljonne, J. P. Calbert, J. L. Brédas, *Adv. Mater.* **2001**, *13*, 1053–1067; b) H. Spanggaard, J. Prehn, M. B. Nielsen, E. Levillain, M. Allain, J. Becher, *J. Am. Chem. Soc.* **2000**, *122*, 9486–9494 and references therein.

[9] J. Roncali, *J. Mater. Chem.* **1997**, *7*, 2307–2321.

[10] I. Jestin, P. Frère, E. Levillain, J. Roncali, *Adv. Mater.* **1999**, *11*, 134–138.

[11] J. F. Favard, P. Frère, A. Riou, A. Benahmed-Gasmi, A. Gorgues, M. Jubault, J. Roncali, *J. Mater. Chem.* **1998**, *8*, 363–366.

[12] E. H. Elandaloussi, P. Frère, A. Riou, J. Roncali, *New J. Chem.* **1998**, 1051–1054.

[13] C. Rovira, J. J. Novoa, *Chem. Eur. J.* **1999**, *5*, 3689–3697.

[14] J. Roncali, L. Rasmussen, C. Thobie-Gautier, P. Frère, H. Brisset, M. Sallé, J. Becher, O. Simonsen, T. K. Hansen, A. Benahmed-Gasmi, J. Orduna, J. Garin, M. Jubault, A. Gorgues, *Adv. Mater.* **1994**, *6*, 841–845.

[15] E. H. Elandaloussi, P. Frère, J. Roncali, P. Richomme, M. Jubault, A. Gorgues, *Adv. Mater.* **1995**, *7*, 390–394.

[16] a) E. Levillain, J. Roncali, *J. Am. Chem. Soc.* **1999**, *121*, 8760–8765; b) J. J. Apperloo, J. M. Raimundo, P. Frère, J. Roncali, R. A. J. Janssen, *Chem. Eur. J.* **2000**, *6*, 2–11.

[17] a) T. K. Hansen, M. V. Lakshmikantham, M. P. Cava, R. E. Niziurski-mann, F. Jensen, J. Becher, *J. Am. Chem. Soc.* **1992**, *114*, 5035; b) A. Benahmed-Gasmi, P. Frère, B. Garrigues, A. Gorgues, M. Jubault, R. Carlier, F. Texier, *Tetrahedron Lett.* **1992**, *33*, 6457–6461.

[18] For reviews of multi-stage redox systems see: a) S. Hünig, H. Berneth, *Top. Curr. Chem.* **1980**, *92*, 1–144; b) K. Deuchert, S. Hünig, *Angew. Chem.* **1978**, *90*, 927–938; *Angew. Chem. Int. Ed. Engl.* **1978**, *17*, 875–886.

[19] D. L. Lichtenberg, R. J. Johnston, K. Hinkelmann, T. Suzuki, F. Wudl, *J. Am. Chem. Soc.* **1990**, *112*, 3302–3307.

[20] a) N. Bellec, K. Boubekeur, R. Carlier, P. Hapiot, D. Lorcy, A. Tallec, *J. Phys. Chem. A* **2000**, *104*, 9750–9759; b) T. Sugimoto, H. Awaji, I. Sugimoto, Y. Misaki, T. Kawase, S. Yoneda, Z. Yoshida, *Chem. Mater.* **1989**, *1*, 535–547.

[21] R. L. Myers, I. Shain, *Anal. Chem.* **1969**, *41*, 980–982.

[22] P. Hapiot, L. D. Kispert, V. V. Konovalov, J. M. Savéant, *J. Am. Chem. Soc.* **2001**, *123*, 6669–6677.

[23] a) L. Martin, S. S. Turner, P. Day, P. Guionneau, J. A. K. Howard, D. E. Hibbs, M. E. Light, M. B. Hursthouse, M. Uruichi, K. Yakushi, *Inorg. Chem.* **2001**, *40*, 1363–1371; b) G. Saito, H. Izukashi, M. Shibata, K. Yoshida, L. A. Kushch, T. Kondo, H. Yamochi, O. O. Drozdova, K. Matsumoto, M. Kusunoki, K. I. Sakaguchi, N. Kojima, E. B. Yagubskii, *J. Mater. Chem.* **2000**, *10*, 893–910.

[24] a) M. Sallé, M. Jubault, A. Gorgues, K. Boubekeur, M. Fourmigué, P. Batail, E. Canadell, *Chem. Mater.* **1993**, *5*, 1196–1198; b) Y. Yamashita, K. Ono, S. Tanaka, K. Imadea, H. Inokuchi, *Adv. Mater.* **1994**, *6*, 295–298; c) P. Frère, K. Boubekeur, M. Jubault, P. Batail, A. Gorgues, *Eur. J. Org. Chem.* **2001**, 3741–3747.


Received: July 26, 2001 [F3441]